Model Based Change Detection of Water Body Using Landsat Imagery: A Case Study of Rajshahi Bangladesh

Tofayel Ahammad*, Hafizur Rahaman, B.M. Refat Faisal, and Nasrin Sultana

Bangladesh Space Research and Remote Sensing Organization (SPARRSO), Sher-e-Bangla Nagar, Agargaon, Dhaka-1207, Bangladesh

ARTICLE INFO

Received: 2 Jan 2020
Received in revised: 12 Jul 2020
Accepted: 17 Jul 2020
Published online: 30 Jul 2020
DOI: 10.32526/ennrj.18.4.2020.33

Keywords:
Water bodies/ Model/ Mosaic/ Pixel/ Binary image

*** Corresponding author:**
E-mail: tofayel.cu.phy@gmail.com

ABSTRACT

This study detected water bodies which included ponds, lakes, rivers, canals, irrigation land, etc. from Landsat TM (Thematic Mapper) and OLI (Operational Land Imager) data by Pixel Based Model (PBM) for the years 2000 to 2018 and identified the change in area of water body. Rajshahi Division of Bangladesh was selected as the study area for this case study. Landsat 5 data acquired in December 18th, 2000, January 12th, 2001, November 14th, 2005, January 26th, 2006, December 23rd, 2010, and December 14th, 2010 along with Landsat 8 data acquired in December 28th, 2015, January 6th, 2016, December 29th, 2018, and November 18th, 2018 were used as satellite imagery for this analysis. Two images of each month were taken to cover study area. The lowest and highest pixel value of the water body for each band was investigated. Then, a Pixel Based Model (PBM) was formed by using the entire Landsat band and run. The output of the model was shown as a binary image which includes water bodies and non-water bodies. The goal of this study is to verify the accuracy in finding common areas, accreted areas and abolished areas of the water bodies using the PBM model. The results show that overall accuracy of the model is 97% for the year 2000 with Kappa 0.94, 97% for the year 2005 with Kappa 0.94, 99% for the year 2010 with Kappa 0.98, 95% for the year 2015 and 2018 with Kappa 0.90. Also, it was observed that there have been significant changes in the water bodies during the chosen time periods.

1. INTRODUCTION

There are many forms of water bodies on the earth surface, such as surface water, lakes, ponds, rivers, reservoirs, transition water (irrigated water), etc. and is an essential component of the hydrological cycle, human beings and other forms of life (Jawak et al., 2015; Chave, 2001; Acharya et al., 2016). Identification of water bodies can be useful in many ways, such as estimation of water areas (Acharya et al., 2016; Rover et al., 2012; Alsdorf et al., 2007), flood area assessment (Acharya et al., 2016; Jain et al., 2005; Chignell et al., 2015), wetland inventories (Acharya et al., 2016; Rebelo et al., 2009; Ozesmi and Bauer, 2014), change detection (Acharya et al., 2016; Rokni et al., 2014; Du et al., 2012), managing and monitoring natural resources (Hassan et al., 2016), environmental monitoring, resource survey and drought detection. Since growing population and increasing socioeconomic necessities creates pressure on land area, the amount and location of water bodies change over time and space (Reis, 2008; Hassan et al., 2016). Changes in the amount and location of water bodies can indicate agricultural and environmental problems and affect human socioeconomic development (Hassan et al., 2016). Accurate estimation of water bodies is essential for both science and engineering research and policy making (Jiang et al., 2014; Selim, 2018; Jaafari and Nazarisamani, 2013; Hassan et al., 2016; Acharya et al., 2016). Satellite based remote sensing is a powerful tool to identify water bodies and detect changes over large areas because it provides continuous snapshots of earth surface over long periods (Reis, 2008). Among other satellite imagery, Landsat satellite imagery is very useful for such study because Landsat TM (Thematic Mapper), OLI (Operational Land Imager) imagery has a high spatial resolution (30 m), provides multispectral images (seven or eleven

Citation: Ahammad T, Rahaman H, Faisal BMR, Sultana N. Model based change detection of water body using Landsat imagery: A case study of Rajshahi Bangladesh. Environ. Nat. Resour. J. 2020;18(4):345-355. (https://doi.org/10.32526/ennrj.18.4.2020.33)

bands), short revisit interval (16 days), decades of records (almost 30 years) and is freely available (Jiang et al., 2014). Thus change detection analysis by using Landsat imagery is no longer cost- prohibitive (Jiang et al., 2014; Nicholas et al., 2013; Verpoorter et al., 2012). In order to detect water bodies, at present, different satellite-derived indices were used. The indices are described in the methodology section.

In this paper, we introduce a Pixel Based Model (PBM) to identify the changed area and identical area of water bodies automatically. The PBM method is more convenient than the water index method in the sense that the PBM method does not need a threshold value to identify water whereas every water index needs a threshold value to identify water. To identify water bodies, the PBM model needs to explore only the highest and lowest pixel value of water bodies. This method is not only useful for water detection but also helpful to detect the changed areas of crops, irrigated land, settlements, forests, etc. Using the PBM model, we detect the water bodies and area changes for the years 2000 to 2018 in the Rajshahi Division of Bangladesh.

2. METHODOLOGY

2.1 Study area

Rajshahi Division is one of the eight administrative divisions of Bangladesh. Geographically, Rajshahi Division is located between 23°48' and 25°16' north latitudes and between 88°01' and 89°48' east longitudes and is situated 23 m above sea level. It has an area of 18,174.4 km² (Miah, 2006). Rajshahi Division is in the central western region of Bangladesh. It consists of eight districts: Bogura, Chapainawabganj, Joypurhat, Naogaon, Natore, Pabna, Rajshahi and Sirajgonj. The famous Padma River borders Rajshahi Division on the south and another famous river, Jamuna River, lies across the eastern border. In the west, Rajshahi Division shares a border with India. This region was chosen because of the wide variety of demographic changes in the region (Miah, 2006). The study area is shown in Figure 1.

2.2. Data acquisition and image processing

To cover the study area, two images are required (path/row-138/43,139/43). Since two images taken on the same date could not be found, two images from the two closest days in December were used. Images were from the years 2000 to 2018 at approximately five year intervals. Landsat 5 TM and Landsat 8 OLI (path 138, row 043 and path 139, row 043) were used in this study. The Landsat 5 TM and Landsat 8 OLI Images were downloaded from USGS Earth Resources Observation Systems Data Centre (Rokni et al., 2014; Sekertekin et al., 2017). The dates of both images of same month were chosen to be as close as possible in the same vegetation season. All visible and infrared bands (except the thermal infrared) were included in the analysis. All the images were projected in UTM Zone 45N. Landsat image processing was performed using ERDAS Imagine 14 (Sekertekin et al., 2017).

Figure 1. Study area

In this paper, Thematic Mapper (TM) and Operational Land Imager (OLI) sensors are used for studying water body's detection for Rajshahi region of Bangladesh. Here, we have used band 1 to 5 for thematic mapper (TM) sensor and band 2 to 7 for Operational Land Imager (OLI) sensor (Rokni et al., 2014; Sekertekin et al., 2017). The data acquisition date and spatial resolution of the satellites sensors used in this paper are shown in Table 1.

2.3. Reference data

For the accuracy assessment of this study, we have used true water pixels which were manually digitized from the Landsat images for the respective years.

2.4. Water index methods

At present to identify water bodies, different water indices have been used. The indices are described in Table 2.

Table 1. Dates of Landsat TM and Landsat OLI satellite image with spatial resolution

Sensor name	Path/Row	Spatial resolution (m)	Image date	Total No. of bands	Number of bands used
Landsat TM	138/043	30	12 Jan 2001	7	6
Landsat TM	139/043	30	18 Dec 2000	7	6
Landsat TM	138/043	30	26 Jan 2006	7	6
Landsat TM	139/043	30	14 Nov 2005	7	6
Landsat TM	138/043	30	23 Dec 2010	7	6
Landsat TM	139/043	30	14 Dec 2010	7	6
Landsat OLI	138/043	30	06 Jan 2016	11	6
Landsat OLI	139/043	30	28 Dec 2015	11	6
Landsat OLI	138/043	30	29 Dec 2018	11	6
Landsat OLI	139/043	30	18 Nov 2018	11	6

Table 2. Satellite derived water index currently used for water detection

Water index	Formula	Threshold	Band information	Reference
Normalized-Difference Water Index (NDWI)	NDWI = (Green − NIR)/(Green + NIR)	There is no fixed threshold value. But it has positive value	For Landsat 5 TM, Band 1=Blue, Band 2=Green, Band 3=Red, Band 4=NIR, Band 5=MIR, Band 7= SWIR For Landsat 8 OLI, Band 2=Blue, Band 3=Green, Band 4=Red, Band 5=NIR, Band 6= MIR, Band 7= SWIR (Rokni et al., 2014).	Mcfeeters (1996); Rokni et al. (2014); Yang et al. (2015); Zhou et al. (2016); Kaplan and Avdan (2017)
Modified Normalized-Difference Water Index (MNDWI)	MNDWI = (Green − MIR)/(Green + MIR)	There is no fixed threshold value. But it has positive value		Xu (2006); Rokni et al. (2014); Yang et al. (2015)
Normalized Difference Moisture Index (NDMI)	NDMI = (NIR − MIR)/(NIR + MIR)	There is no fixed threshold value. But it has positive value		Wilson and Sader (2002); Rokni et al. (2014)
Water Ratio Index (WRI)	WRI = (Green + Red)/ (NIR + MIR)	There is no fixed threshold value. But value of water is greater than 1		Shen and Li (2010); Rokni et al. (2014)
Normalized Difference Vegetation Index (NDVI)	NDVI = (NIR − Red)/ (NIR + Red)	There is no fixed threshold value. But it has negative value		Trishchenko et al. (2001); Hatfield and Prueger 2010); Zoran and Stefan (2006)
Automated Water Extraction Index (AWEI)	AWEI = 4 × (Green-MIR) − (0.25 × NIR + 2.75 × SWIR)	There is no fixed threshold value. But value of water is greater than 1		Feyisa et al. (2014); Rokni et al. (2014)

2.5. Pixel based model for water detection

At first, all the obtained images were converted to spectral radiance using ERDAS IMAGINE 14 model maker. The required information including data acquisition date, Gain (Radiance_Multi_Band_x) and Bias (Radiance_Add_Band_x) was obtained from Landsat header files (Rokni et al., 2014). The lowest and highest pixel value (radiance value) of the water body for each band of the remotely sensed image 2000, 2005, 2010, 2015, and 2018 was identified by the selection of minimum and maximum value of each image band. The lowest and highest pixel value of water body for the images from 2000, 2005, 2010, 2015, and 2018 is shown in Table 3, Table 4, Table 5, Table 6, and Table 7, respectively. Then a Pixel Based Model (PBM) was formed indicating lowest and highest pixel value for each band for the year 2000. The result shows a binary image which includes only a water body and a non-water body.

Table 3. Lowest and highest pixel value of the water body for the image 2000

Band number	Lowest pixel value (radiance value)	Highest pixel value (radiance value)
1	48	64
2	33	54
3	25	42
4	5	24
5	1	6
7	1	2

Table 4. Lowest and highest pixel value of the water body for the image 2005

Band number	Lowest pixel value (radiance value)	Highest pixel value (radiance value)
1	51	72
2	39	60
3	21	47
4	15	29
5	1	5
7	1	2

Table 5. Lowest and highest pixel value of the water body for the image 2010

Band number	Lowest pixel value (radiance value)	Highest pixel value (radiance value)
1	58	74
2	44	63
3	29	53
4	16	29
5	1	11
7	1	3

Table 6. Lowest and highest pixel value of the water body for the image 2015

Band number	Lowest pixel value (radiance value)	Highest pixel value (radiance value)
2	63	73
3	44	57
4	29	44
5	12	31
6	1	6
7	1	2

Table 7. Lowest and highest pixel value of the water body for the image 2018

Band number	Lowest pixel value (radiance value)	Highest pixel value (radiance value)
2	58	75
3	42	62
4	28	47
5	11	33
6	1	11
7	1	3

The same procedure was repeated for remotely sensed images from 2005, 2010, 2015, and 2018. The results from the above five model identify water bodies for the years 2000, 2005, 2010, 2015, and 2018 respectively. Then a new model was made to detect the water bodies that were present in 2000 but abolished in 2005 by subtracting the binary image of 2005 from that of 2000. Another model was made to detect the accreted area of water bodies in 2005 but absent in 2000 by subtracting binary image of 2000 from that of 2005.

The PBM used for detecting water bodies is shown below using the pseudo-code defined by ERDAS software:

```
EITHER 1 IF (
(Band 1 >= lowest pixel value AND
Band 1 <= highest pixel value) AND
(Band 2 >= lowest pixel value AND
Band 2 <= highest pixel value) AND
(Band 3 >= lowest pixel value AND
Band 3 <= highest pixel value) AND
(Band 4 >= lowest pixel value AND
Band 4 <= highest pixel value) AND
(Band 5 >= lowest pixel value AND
Band 5 <= highest pixel value) AND
(Band 6 >= lowest pixel value AND
Band 6 <= highest pixel value) AND
) OR 0 OTHERWISE
```

Lastly, a model was made to detect the identical area of water bodies which are present both in 2000 and 2005 by subtracting the last two binary images from any of the binary image of water body. A flow chart of the work is shown in Figure 2. The model used in the whole work has been shown in the following:

Model for detecting abolished area in 2005 (Model-3 in the flowchart): Model for water bodies 2000 - Model for water bodies 2005

Model for detecting accreted area in 2005 (Model-4 in the flowchart): Model for water bodies 2005 - Model for water bodies 2000

Model for Identical water body which is present both in 2000 and 2005 (Model-5 in the flowchart): Water bodies' 2000 or Water bodies 2005 - abolished area in 2005 - accreted area in 2005

Model for detecting abolished area in 2010 (Model-3 in the flowchart): Model for water bodies 2005 - Model for water bodies 2010

Model for detecting accreted area in 2010 (Model-4 in the flowchart): Model for water bodies 2010 - Model for water bodies 2005

Model for Identical water body which is present both in 2005 and 2010 (Model-5 in the flowchart): Water bodies' 2000 or Water bodies 2010 - abolished area in 2010 - accreted area in 2010

Model for detecting abolished area in 2015 (Model-3 in the flowchart): Model for water bodies 2010 - Model for water bodies 2015

Model for detecting accreted area in 2015 (Model-4 in the flowchart): Model for water bodies 2015 - Model for water bodies 2010

Model for Identical water body which is present both in 2010 and 2015 (Model-5 in the flowchart): Water bodies' 2010 or Water bodies 2015 - abolished area in 2015 - accreted area in 2015

Model for detecting abolished area in 2018 (Model-3 in the flowchart): Model for water bodies 2015 - Model for water bodies 2018

Model for detecting accreted area in 2018 (Model-4 in the flowchart): Model for water bodies 2015 - Model for water bodies 2018

Model for Identical water body which is present both in 2015 and 2018 (Model-5 in the flowchart): Water bodies' 2015 or Water bodies 2018 - abolished area in 2018 - accreted area in 2018

Model for Identical water body which is present from 2000 to 2018 (Model-5 in the flowchart): Water bodies' 2000 or Water bodies 2005 or Water bodies 2010 or Water bodies 2015 or Water bodies 2018 - abolished area in 2005 - accreted area in 2005 - abolished area in 2010 - accreted area in 2010 - abolished area in 2015 - accreted area in 2015 - abolished area in 2018 - accreted area in 2018

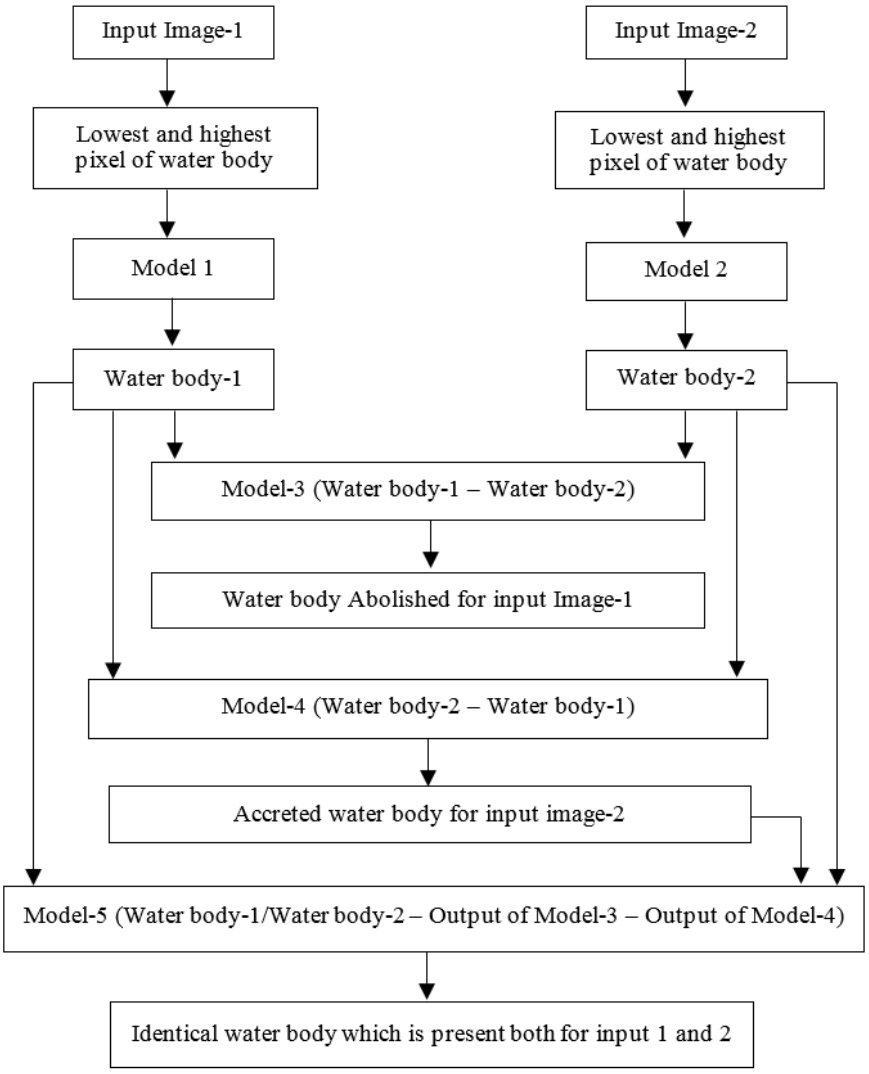

Figure 2. Overall flowchart adopted in this study

3. RESULTS AND DISCUSSION

Landsat TM (2010) and Landsat OLI (2017) images were used in this study. In this paper, a Pixel Based Model was investigated to detect the water bodies and its changes from the year 2000 to 2018 with five year interval. Figure 3(a), Figure 3(b), Figure 3(c), Figure 3(d), and Figure 3(e) show the false color composite (543) images of Rajshahi division for the year 2000, 2005, 2010, 2015 and 2018, respectively. Figure 3(f), Figure 3(g), Figure 3(h), Figure 3(i), and Figure 3(j) show the water body area for the year 2000, 2005, 2010, 2015, and 2018, respectively.

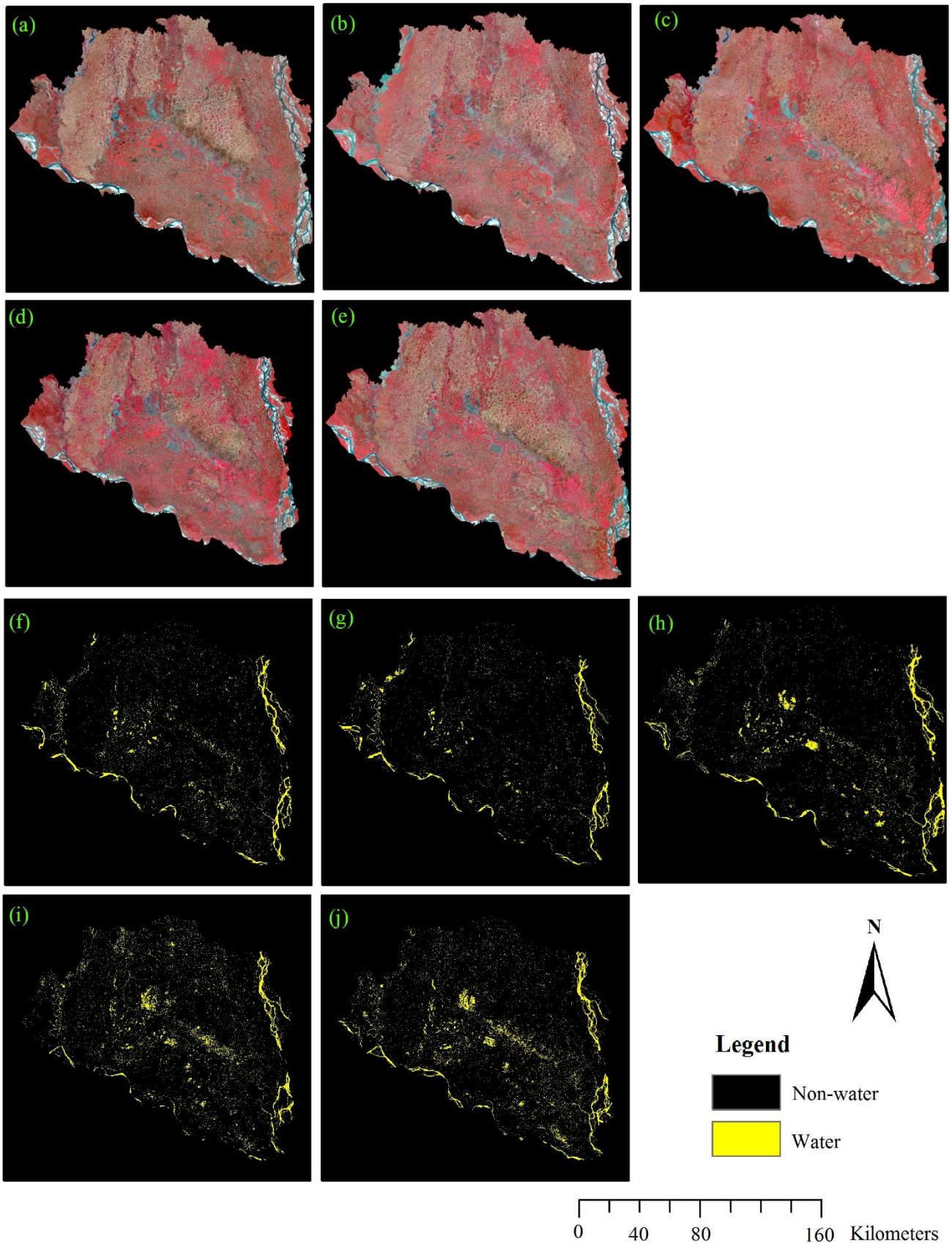

Figure 3. (a) Input satellite image 2000; (b) Input satellite image 2005; (c) Input satellite image 2010; (d) Input satellite image 2015; (e) Input satellite image 2018; (f) Detected water body 2000; (g) Detected water body 2005; (h) Detected water body 2010; (i) Detected water body 2015; (j) Detected water body 2018.

The accuracy of the PBM model was tested for the whole study period. The overall accuracy of the model is 97% for the year 2000 with Kappa 0.94. Similarly overall accuracy of the model is 97% for the year 2005 with Kappa 0.94, 99% for the year 2010 with Kappa 0.98, 95% for the year 2015 and 2018 with Kappa 0.90. The accuracy of the PBM model is shown in Table 8.

Table 8. Accuracy of the PBM model

Accuracy (%)				
Year	User	Producer	Overall	Kappa
2000	96.08	98	97	0.94
2005	94.34	100	97	0.94
2010	100.00	98	99	0.98
2015	94.12	96	95	0.90
2018	94.12	96	95	0.90

The increment and decreases of the water body is due to the erosion, accretion and net gain/loss of land in the Coastal Areas, formation of new houses, and formation of new fishing zones in the study area. The area which is eroded creates millions of environmental refuges whereas the area which is accreted give shelter to millions of environmental refuges (Alam and Uddin, 2013). The statistics revealed that water body and non-water body types were consistent in their direction of change from 2000 to 2018. The total area of water bodies was 808.59 km^2 in 2005 which is least during the study period and the highest (1373.77 km^2) is in 2018, showing continuous increment of water body from 2000 to 2018 (shown in Table 9).

In 2000, water body covers 5.35% of the total study area. In 2005, water body has been decreased to 4.45% of the total area with a net change of 0.90% (163.44 km^2) from the year 2000. From 2010, there was a continuous increase of water body up to 2018.

In 2010, water body increased to 5.55% of the total area with a net change of 1.10 % (199.55 km^2) from the year 2005. In 2015, water body increased to 6.74% of the total area with a net change of 1.19% from the year 2010. In 2018, water body increased to 7.56% of the total area with a net change of 0.82% from the year 2015. In comparison with the base year 2000, water bodies increased to 2.21% in 2018. The percentage of water body and non-water body from year 2000 to 2018 and variation of water body from year 2000 to 2018 has been shown in Figure 4 and Figure 5, respectively.

Table 9. Area of water body and its change from the year 2000 to 2018

Year	Area of water body (km^2)	Abolished area of water body (km^2)	Accreted area of water body (km^2)	Net Change (km^2)
2000	972.03	-	-	-
2005	808.59	559.98	396.53	-163.45
2010	1008.14	401.07	600.62	199.55
2015	1225.42	546.55	763.83	217.28
2018	1373.77	553.75	702.10	148.35

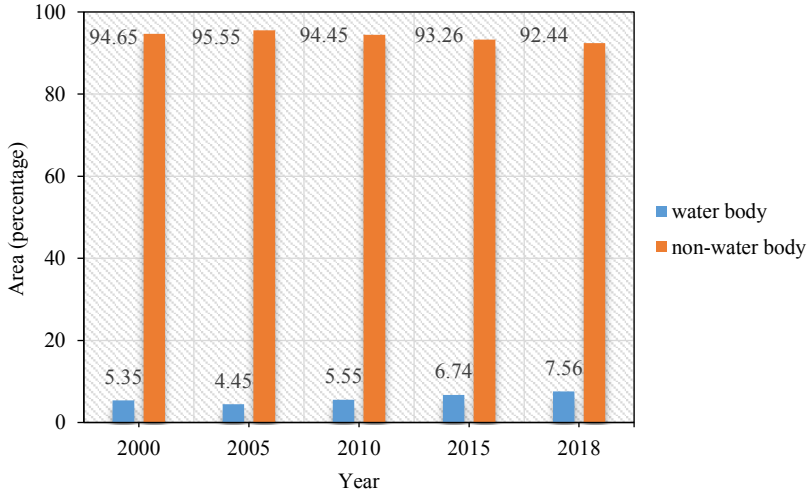

Figure 4. Percentage of water body and non-water body from 2000 to 2018

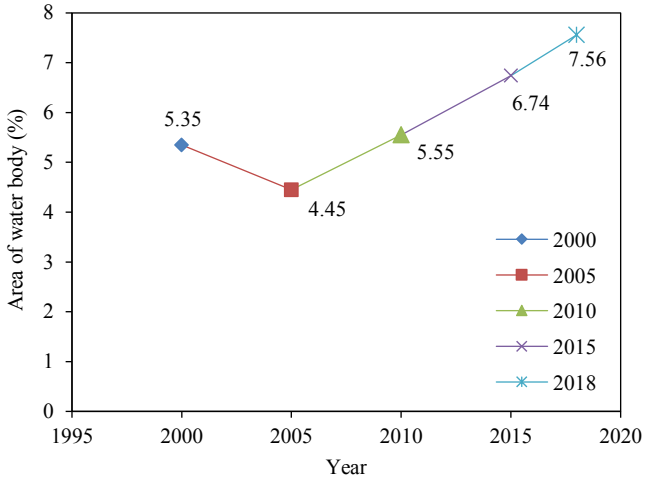

Figure 5. Variation of water body from 2000 to 2018

In 2005, 559.98 km^2 of water body had been abolished and 396.53 km^2 new areas has been added to water body with a net decrease of 163.45 km^2 water body. In 2010, 401.07 km^2 area of water body had been abolished and 600.62 km^2 of new areas was added to water body with a net increase of 199.55 km^2 water body. In 2015, 546.55 km^2 of water body had been abolished and 763.83 km^2 of new areas was added to water body with a net increase of 217.28 km^2 water body. In 2018, 553.75 km^2 area of water body had been abolished and 702.10 km^2 of new areas was added to water body with a net increase of 148.35 km^2 water body. From the above discussion it is clear that accreted area of water body has been increased every year except 2005 which implies that erosion has been increased every year after 2005. Due to erosion there is a huge probability to create new environmental refuges. Area of water body and its change from the year 2000 to 2018 has been shown in Table 9. Figure 6(a), Figure 6(c), Figure 6(e), and Figure 6(g) show the abolished area of water body for the years 2005, 2010, 2015 and 2018, respectively. Figure 6(b), Figure 6(d), Figure 6(f), and Figure 6(h) show the accreted area of water body for the years 2005, 2010, 2015, and 2018, respectively.

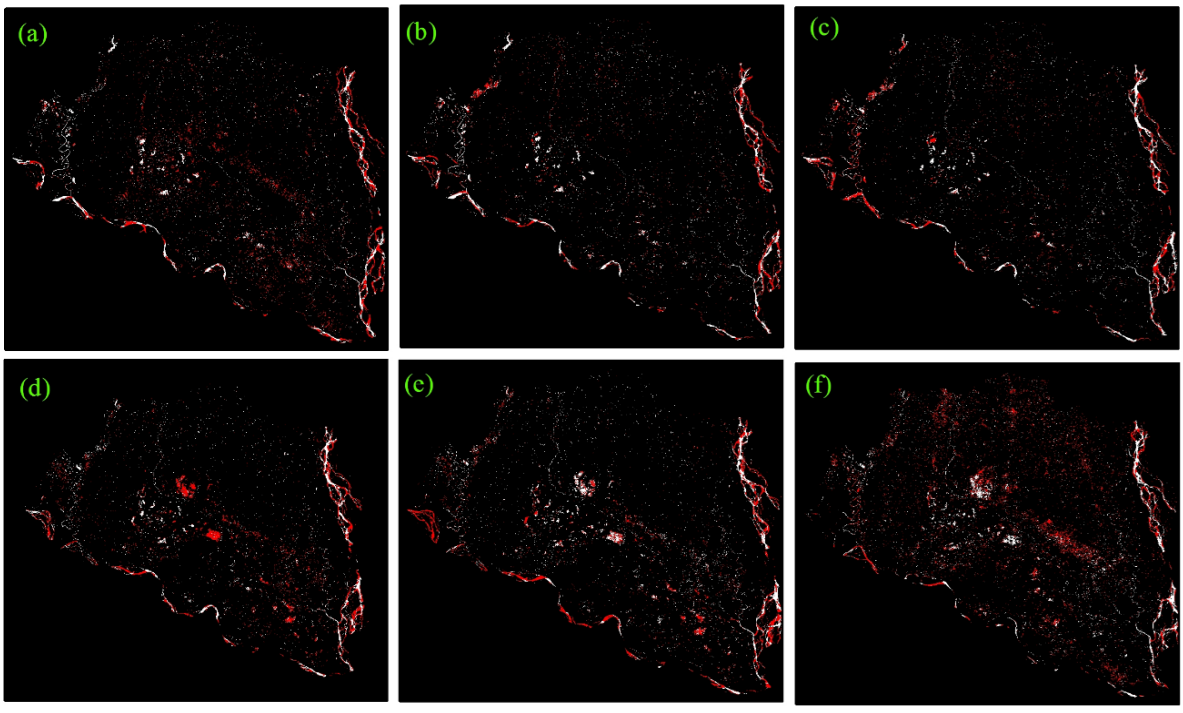

Figure 6. (a) Abolished area of water body 2005; (b) Accreted area of water body 2005; (c) Abolished area of water body 2010; (d) Accreted area of water body 2010; (e) Abolished area of water body 2015; (f) Accreted area of water body 2015; (g) Abolished area of water body 2018; (h) Accreted area of water body 2018

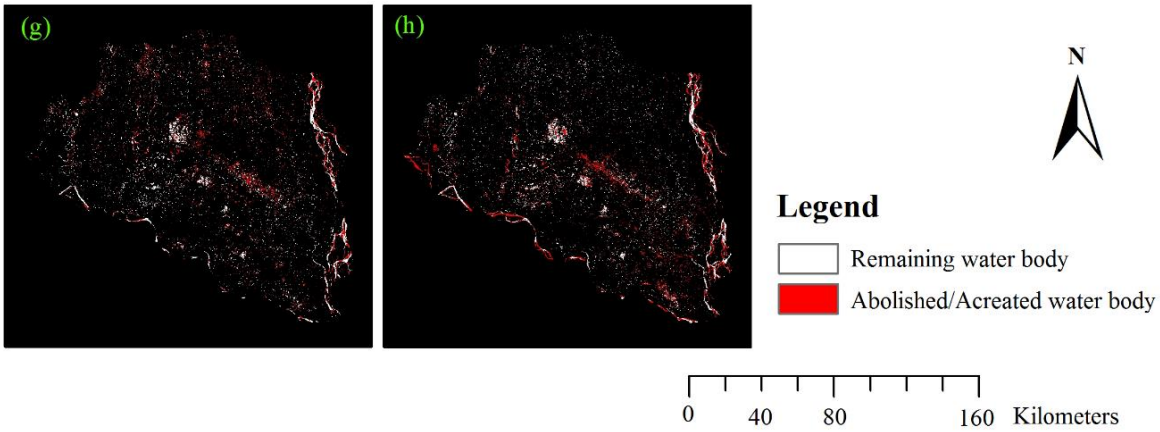

Figure 6. (a) Abolished area of water body 2005; (b) Accreted area of water body 2005; (c) Abolished area of water body 2010; (d) Accreted area of water body 2010; (e) Abolished area of water body 2015; (f) Accreted area of water body 2015; (g) Abolished area of water body 2018; (h) Accreted area of water body 2018 (cont.).

The identical areas of water body from year 2000 to 2005, 2005 to 2010, 2010 to 2015, and 2015 to 2018 are 412.06, 407.52, 461.59 and 671.67 km^2 respectively (Table 10). But in comparison with the base year 2000, only 78.21 km^2 of water body was identical with 2018 which shows that erosion and accretion are common hazards in this region. Figure 7(a), Figure 7(b), Figure 7(c), Figure 7(d), and Figure 7(e) show the identical area of water body for the range of year 2000 to 2005, 2005 to 2010, 2010 to 2015, 2015, to 2018, and 2000 to 2018, respectively.

Table 10. Identical area of water body from the year 2000 to 2018

Year range	Identical area (ha)	Identical area (km^2)
2000 to 2005	41,205.7	412.06
2005 to 2010	40,751.6	407.52
2010 to 2015	46,159.2	461.59
2015 to 2018	67,167.1	671.67
2000 to 2018	7,821.09	78.21

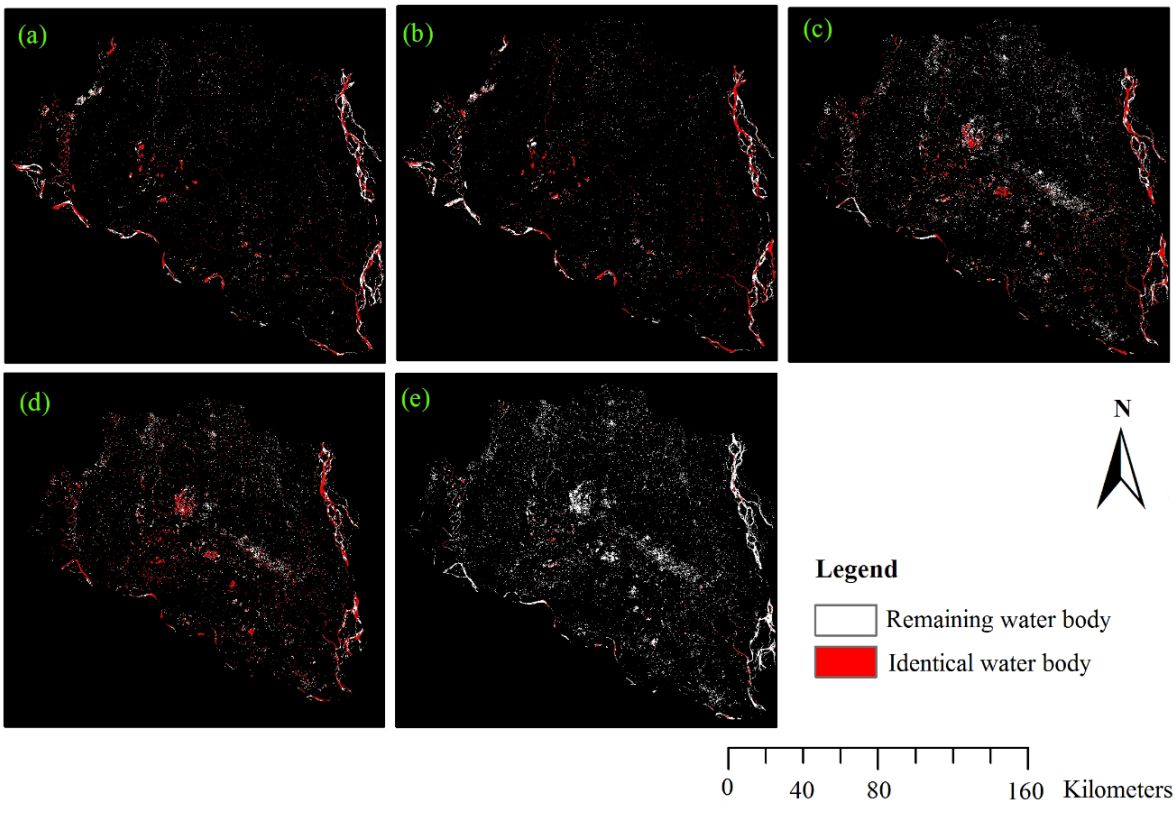

Figure 7. (a) Identical water body present 2000 and 2005; (b) Identical water body present 2005 and 2010; (c) Identical water body present 2010 and 2015; (d) Identical water body present 2015 and 2018; (e) Identical water body from 2000 to 2018

4. CONCLUSION

The present study demonstrates a Pixel Based Model technique to detect water bodies using Landsat satellite imagery for the years 2000 to 2018. This study also finds abolished area, accreted area and identical area of water body using PBM method for the study period. The PBM model has high accuracy for this analysis and it is very convenient to detect water body, abolished area, accreted area and identical area in relatively short time. This method is also very useful in the sense that this model needs to explore lowest and highest pixel value (radiance value) of the water body for each band of the remotely sensed image by the selection of minimum and maximum value of each image band. The result showed that the accreted area of water body in Rajshahi Division of Bangladesh has increased every year except 2005 which implies that erosion is a dominant phenomenon is this region. Due to erosion, there is a huge probability to create new environmental refuges. Regular analysis is required to get the exact condition of this area. If the government gets the real information about the erosion and accretion, it will be very helpful for the government to take immediate proper steps to resolve the problems. This method is not only useful for water detection but also helpful to detect crops, irrigated land, settlement, forest, etc.

REFERENCES

Alam MS, Uddin K. A Study of morphological changes in the coastal areas and Offshore Islands of Bangladesh using remote sensing. Scientific and Academic Publishing 2013;2(1):15-8.

Alsdorf DE, Rodríguez E, Lettenmaier DP. Measuring surface water from space. Reviews of Geophysics 2007;45(2): RG2002(1-24).

Acharya TD, Lee DH, Yang IT, Lee JK. Identification of water bodies in a Landsat 8 OLI image using a J48 decision tree. Sensors 2016;16:1075.

Chave P. The EU water framework directive: An introduction. IWA Publishing; 2001. p. 208.

Chignell SM, Anderson RS, Evangelista PH, Laituri MJ, Merritt DM. Multi-temporal independent component analysis and Landsat 8 for delineating maximum extent of the 2013. Colorado Front Range Flood. Remote Sensing 2015;7:9822-43.

Du Z, Linghu B, Ling F, Li W, Tian W, Wang H, Gui Y, Sun B, Zhang X. Estimating surface water area changes using time-series Landsat data in the Qingjiang River Basin, China. Journal of Appllied Remote Sensing 2012;6:063609.

Feyisa GL, Meilby H, Fensholt R, Proud SR. Automated water extraction index: A new technique for surface water mapping using Landsat imagery. Remote Sensing of Environment 2014;140:23-35.

Hatfield JL, Prueger JH. Value of using different vegetation indices to quantify agricultural crop characteristics at different growth stages under varying management practices. Remote Sensing 2010;2:562-78.

Hassan Z, Shabbir R, Ahmad SS, Malik AH, Aziz N, Buttand A, Erum S. Dynamics of land use and land cover change (LULCC) using geospatial techniques: A case study of Islamabad Pakistan. Springer Plus 2016;5,812(1-11).

Jiang H, Feng M, Zhu Y, Lu N, Huang J, Xiao T. An automated method for extracting rivers and lakes from Landsat imagery. Remote Sensing 2014;6:5067-89.

Jain S, Singh RD, Jain MK, Lohani AK. Delineation of flood-prone areas using remote sensing techniques. Water Resource Management 2005;19:333-47.

Jaafari S, Nazarisamani A. comparison between land use/land cover mapping through Landsat and Google Earth Imagery. American-Eurasian Journal of Agricultural and Environmental Sciences 2013;13(6):763-68.

Jawak SD, Kulkarni K, Luis AJ. A review on extraction of lakes from remotely sensed optical satellite data with a special focus on Cryospheric Lakes. Advances in Remote Sensing 2015;4:196-213.

Kaplan G, Avdan U. Object-based water body extraction model using Sentinel-2 satellite imagery. European Journal of Remote Sensing 2017;50:137-43.

Mcfeeters SK. The use of the normalized difference water index (NDWI) in the delineation of open water features. International Journal of Remote Sensing 1996;17:1425-32.

Miah S. Rajshahi Division [internet]. 2006 Available from: http://en.banglapedia.org/index.php?title=Rajshahi_Division.

Nicholas R, Goodwin, Lisa JC, Robert JD, Flood N, Tindall D. Cloud and cloud shadow screening across Queensland, Australia: An automated method for Landsat TM/ETM+ time series. Remote Sensing of Environment 2013;134:50-65.

Ozesmi SL, Bauer ME. Satellite remote sensing of wetlands. Wetlands Ecological Management 2014;10:381-402.

Reis S. Analyzing land use/land cover changes using remote sensing and GIS in Rize, North-East Turkey. Sensors 2008;8:6188-202.

Rokni K, Ahmad A, Selamat A, Hazini S. Water feature extraction and change detection using Multitemporal Landsat Imagery. Remote Sensing 2014;6:4173-89.

Rover J, Ji L, Wylie BK, Tieszen LL. Establishing water body areal extent trends in interior Alaska from multi-temporal Landsat data. Remote Sensing Letters 2012;3:595-604.

Rebelo LM, Finlayson CM, Nagabhatla N. Remote sensing and GIS for wetland inventory, mapping and change analysis. Journal of Environmental Management 2009;90:2144-53.

Shen L, Li C. Water Body Extraction from Landsat ETM+ Imagery Using Adaboost Algorithm. Proceedings of 18th International Conference on Geoinformatics; Beijing: China; 2010. p. 1-4.

Selim M. Change Detection Analysis using new nano satellite imagery. International Journal of Engineering and Advanced Technology 2018;7:1-10.

Sekertekin A, Marangoz AM, Akcin H. Pixel-based classification analysis of land use land cover using Sentinel-2 and Landsat-8 data. International Archives of the Photogrammetry, Remote Sensing and Spatial Information Sciences 2017;XLII-4/W6: 91-3.

Trishchenko AP, Cihlar J, Zhanqing Li. Effects of spectral response function on surface reflectance and NDVI measured with moderate resolution satellite sensors. Remote Sensing of Environment 2001;81:1-18.

Verpoorter C, Kutser T, Tranvik L. Automated mapping of water bodies using Landsat multispectral data. Limnology and Oceanography: Methods 2012;10:1037-50.

Wilson EH, Sader SA. Detection of forest harvest type using multiple dates of Landsat TM imagery. Remote Sensing of Environment 2002;80:385-96.

Xu H. Modification of normalised difference water index (NDWI) to enhance open water features in remotely sensed imagery. International Journal of Remote Sensing 2006;27:3025-33.

Yang L, Tian S, Yu L, Ye F, Qian J, Qian Y. Deep learning for extracting water body from Landsat imagery. International Journal of Innovative Computing, Information and Control 2015;11:1913-29.

Zoran M, Stefan S. Climatic Changes Effects on Spectral Vegetation Indices for Forested Areas Analysis from Satellite Data. Proceedings of the 2nd Environmental Physics Conference; Alexandria: Egypt; 2006. p. 73-83.

Zhou ZG, Tang P, Zhou M. Detecting anomaly regions in satellite image time series based on seasonal autocorrelation analysis. ISPRS Annals of the Photogrammetry, Remote Sensing and Spatial Information Sciences 2016;III-3:303-10.